Plant Biotechnology Journal
Open Access

Plant Biotechnology Journal (2023), pp. 1–14 doi: 10.1111/pbi.14226

MicroRNA482/2118 is lineage-specifically involved in gibberellin signalling via the regulation of *GID1* expression by targeting noncoding *PHAS* genes and subsequently instigated phasiRNAs

Yanqing Zhang[1,2,3], Zaohai Zeng[1,2,3], Huimin Hu[1,2,3], Minglei Zhao[1,2,3], Chengjie Chen[1,2,3], Xingshuai Ma[1,2,3], Guanliang Li[1,2,3], Jianguo Li[1,2,3], Yuanlong Liu[1,2,3], Yanwei Hao[1], Jing Xu[1,2,3,*] and Rui Xia[1,2,3,*]

[1]*State Key Laboratory for Conservation and Utilization of Subtropical Agro-Bioresources, College of Horticulture, South China Agricultural University, Guangzhou, China*

[2]*Guangdong Laboratory for Lingnan Modern Agriculture, South China Agricultural University, Guangzhou, China*

[3]*Key Laboratory of Biology and Germplasm Enhancement of Horticultural Crops in South China, Ministry of Agriculture and Rural Affairs, South China Agricultural University, Guangzhou, China*

Received 15 June 2023;
revised 5 October 2023;
accepted 22 October 2023.
**Correspondence* (Tel +86-20-38348652; fax +86-20-85280228; email jxu@scau.edu.cn; Tel +86-20-38348652; fax +86-20-85280228; email rxia@scau.edu.cn)

Keywords: miR482/2118, *LcTASL*, phasiRNA, *LcGID1*, gibberellin signalling, seed development.

Summary

MicroRNA482/2118 (miR482/2118) is a 22-nt miRNA superfamily, with conserved functions in disease resistance and plant development. It usually instigates the production of phased small interfering RNAs (phasiRNAs) from its targets to expand or reinforce its silencing effect. Using a new high-quality reference genome sequence and comprehensive small RNA profiling, we characterized a newly evolved regulatory pathway of miR482/2118 in litchi. In this pathway, miR482/2118 cleaved a novel noncoding *trans*-acting gene (*LcTASL1*) and triggered phasiRNAs to regulate the expression of gibberellin (GA) receptor gene *GIBBERELLIN INSENSITIVE DWARF1* (*GID1)* in *trans*; another *trans*-acting gene *LcTASL2*, targeted by *LcTASL1*-derived phasiRNAs, produced phasiRNAs as well to target *LcGID1* to reinforce the silencing effect of *LcTASL1*. We found this miR482/2118-*TASL*-*GID1* pathway was likely involved in fruit development, especially the seed development in litchi. *In vivo* construction of the miR482a-*TASL*-*GID1* pathway in *Arabidopsis* could lead to defects in flower and silique development, analogous to the phenotype of *gid1* mutants. Finally, we found that a GA-responsive transcription factor, LcGAMYB33, could regulate *LcMIR482/2118* as a feedback mechanism of the sRNA-silencing pathway. Our results deciphered a lineage-specifically evolved regulatory module of miR482/2118, demonstrating the high dynamics of miR482/2118 function in plants.

Introduction

Small RNAs (sRNAs), a class of short regulatory RNAs of 20–24 nucleotides (nt) in length, are essential for plant development and environmental adaption mainly via post-transcriptionally gene silencing (PTGS) (Borges and Martienssen, 2015; C. Chen *et al*., 2018). According to the feature of biogenesis and function, plant sRNAs are classified as microRNA (miRNA) and short interfering small RNA (siRNA) (Axtell, 2013). MiRNAs pair with their target genes and induce gene silencing through either transcript cleavage or translation inhibition (Achkar *et al*., 2016; Voinnet, 2009; Yu *et al*., 2017). In some cases, after the induced cleavage, miRNAs induce the generation of secondary phased siRNAs (phasiRNAs) from their target genes (Allen *et al*., 2005; Liu *et al*., 2020; Yoshikawa *et al*., 2005). PhasiRNAs are involved, at the post-transcriptional level similar to miRNAs, in diverse biological processes in plants (Liu *et al*., 2020). On one hand, phasiRNAs can act in *cis* to cleave their precursors and homologs to enhance the silencing effect of miRNAs; on the other hand, they can function in *trans* to regulate genes other than the parental genes to further expand the functions of miRNAs (Jiang *et al*., 2020; Liu *et al*., 2020; Tamim *et al*., 2018; Zhang *et al*., 2020).

MircroRNA482/2118 (miR482/2118), a 22-nt miRNA superfamily consisting of two subfamilies, miR482 and miR2118, targets a large range of genes and triggers the production of 21-nt phasiRNAs, which is widespread and conserved in seed plants (Komiya, 2017; Zhang *et al*., 2021). It mainly targets hundreds of *NUCLEOTIDE BINDING SITE-LEUCINE-RICH REPEATS* (*NBS-LRRs*), generating phasiRNAs to regulate disease defence in gymnosperms and eudicots, while triggers the production of phasiRNAs from hundreds of long noncoding RNAs (lncRNAs) involved in plant reproduction in monocots (Xia *et al*., 2015; Zhai *et al*., 2011; Zhang *et al*., 2021). In eudicots, in addition to targeting *NBS-LRRs*, some species- or lineage-specific functions of miR482/2118 have been evolved (Canto-pastor *et al*., 2019; Tang *et al*., 2020). For example, a tomato specific lncRNA *TAS5* endows miR2118b a subfunction in disease defence (Canto-pastor *et al*., 2019). And in litchi, miR2118 negatively affects fruit

Please cite this article as: Zhang, Y., Zeng, Z., Hu, H., Zhao, M., Chen, C., Ma, X., Li, G., Li, J., Liu, Y., Hao, Y., Xu, J. and Xia, R. (2023) MicroRNA482/2118 is lineage-specifically involved in gibberellin signalling via the regulation of *GID1* expression by targeting noncoding *PHAS* genes and subsequently instigated phasiRNAs. *Plant Biotechnol. J*., https://doi.org/10.1111/pbi.14226.

storability via targeting an energy-related gene encoding calcium ATPase (Ca^{2+}-ATPase) (Tang *et al*., 2020). Recently, it was found that miR2118 could, in several eudicots such as flax, strawberry and columbine, induce the biogenesis of abundant 21-nt phasiRNAs in pre-meiotic anther, likely regulating reproductive development as it does in monocots (Pokhrel *et al*., 2021).

The hormone gibberellin (GA) is a prominent hormone in modulating diverse plant developmental processes including seed germination and development, flower development and fruit initiation (Arnaud *et al*., 2010; Gao and Chu, 2020; Tyler *et al*., 2004). When bioactive GAs are present, GAINSENSITIVE DWARF1 (GID1) perceives GAs leading to a conformational change, which induces the interaction with negative regulator DELLA and results in DELLA degradation by a 26S proteasome, releasing the downstream GA-activated genes (Gao and Chu, 2020). In Arabidopsis, AtGID1A played a major role during fruit set and growth, whereas AtGID1B and AtGID1C had specific roles in seed development and pod elongation, respectively (Gallego-Giraldo *et al*., 2014). It has been shown that GA signalling was post-transcriptionally regulated by several miRNAs, including miR156 and miR159 (Yu and Wang, 2020). miR156 and miR159 mediated GA signalling through their targeted *SPLs* and *GAMYBs* interacted with DELLA proteins; once DELLA degradation induced by GA perception, releasing of *SPLs* promoted the floral transition while *GAMYBs* affected flower development, fruit parthenocarpy and development such as fruit set (da Silva *et al*., 2017; Tsuji *et al*., 2006; Wang *et al*., 2018; Yu *et al*., 2012; Yu and Wang, 2020; Zhao *et al*., 2018).

Litchi (*Litchi chinensis* Sonn.) is an economically important fruit tree in South Asia. Seed size is a critical agronomic trait, with smaller seed or seedless being a desirable feature for commercial breeding. Some litchi varieties produce a proportion of aborted seeds and thus have a higher flesh recovery (Wang *et al*., 2017). How this seed abortion occurs remains elusive. It is well-documented that GA is an essential hormone for seed formation and development in plants (Kim *et al*., 2005; Kozaki and Aoyanagi, 2022; Serrani *et al*., 2007). The GA content of normal-seeded cultivars is often higher than the cultivars with aborted seed, and the ratio of promoting hormone (IAA + GAs + CTKs) and inhibiting hormone ABA is higher in normal seed varieties, indicating that the disorder of endogenous hormones may be the cause of litchi seed abortion (Huang, 2001; Qiu *et al*., 1998). Recently, we found, in litchi, miR482/2118 has gained a variety of new functions via regulating many litchi-specific target genes. One of these genes showing great sequence similarity to the GA receptor *GID1* produces ample phasiRNAs (Ma *et al*., 2018). It implies that miR482/2118 might be involved in GA signalling in litchi directly by the adoption of a new target gene. In this study, taking advantage of our newly published high-quality litchi genome and multi-omics data, we characterized two miR482/2118 targeted noncoding genes, which produced phasiRNAs to target *GID1* in litchi. Our experimental evidence demonstrated that this newly evolved miR482/2118-*TASL*-*GID1* pathway was involved in seed development and this regulatory module was under a feedback regulation of GA signalling in litchi.

Results

Revisiting the miR482/2118 family and their targets in litchi

We have previously characterized seven members of miR482/2118 in litchi based on a draft scaffold-level genome (Ma *et al*., 2018). To get a complete view of the functional diversity of miR482/2118, here, in combination with a new high-quality chromosomal-level reference genome sequence (Hu *et al*., 2022) and more small RNA sequencing data from different tissues, a total of 12 miR482/2118 members were identified from 13 loci of the litchi genome (Table S1), with *LcMIR482g* and *LcMIR482f* producing mature miRNAs with identical sequences (Figure S1). According to the classification of miR482/2118 members in a previous study (Shivaprasad *et al*., 2012), there are six miR482-type members (starting with 'UC') and six miR2118-type (with a 2-nt shift backward) in litchi (Figure 1a). Ten *MIR482/2118* gene loci generated mature miRNA from the 3′ arm of their precursor, while three mature miRNAs (Lc-miR482b, Lc-miR482d, Lc-miR482e) were generated from the 5′ arm (Table S1, Figure S1). Mature miR482/2118 sequences are more conserved compared to the star sequences, and there is a conserved bulge (asymmetrical mismatch) at the 10th position of the miR482-type sequence, which confers the mature sequence of miR482/2118 a length of 22-nt (Figure 1b). In addition, miR482/2118s are distributed on six different chromosomes, with a clear cluster phenomenon on chromosomes 6, 7 and 14, especially on chromosome 14 (Figure 1c).

To further explore the functions of miR482/2118 family, we re-analysed its target genes using the newly updated genome. A total of 47 annotated target genes were identified, among which 19 genes belonged to the *NBS-LRR* family, 13 genes of unknown functions, and others including genes homologous to kinases, hormone response proteins, calcium transport proteins, etc. (Table S2). As miR482/2118 is capable of triggering downstream phasiRNA production, we also characterized 43 *PHAS* loci targeted by miR482/2118 and generating 21-nt phasiRNAs (Phasing score ≥ 10) (Table S3). Among them, 23 *PHAS* loci overlap protein-coding genes, with most *PHAS* genes belonging to disease-resistance protein (Figure 1d,e; Table S3). Distribution of these 23 *PHAS* target genes also showed clusters phenomenon on chromosomes (Figure 1c), for instance, a supercluster of seven target genes, all of which are disease-resistance and stress-resistance related genes, was present on chromosome 4. Both the miR482/2118s and phasiRNAs generated from the aforementioned 23 loci showed organ-preferential enrichment, as previously reported Ma *et al*. (2018), with many of them highly expressed in vegetative tissues, while a few miRNA and *PHAS* loci specifically accumulated in other organs, like flower and fruits (Figure S2).

Neofunctionalisation of Lc-miR482/2118 in the repression of gibberellin signalling receptor *LcGID1* via phasiRNA derived from noncoding *PHAS* genes

In our previous study (Ma *et al*., 2018), we proposed that miR482/2118 has evolved some lineage- and species-specific functions in litchi via new target gene acquisition, in addition to the target genes related to disease and stress resistance (Figure 1e; Tables S2 and S3). When we further checked these litchi-specific *PHAS* genes targeted by miR482/2118, the *PHAS19* gene (*LITCHI007943*) aroused our interest. *PHAS19* is located on chromosome 11 with five exons, and produced profuse phasiRNAs after the cleavage directed by miR482/2118 (Figure 2a). Consistent with the 2-nt shift of miR482 in contrast to miR2118 type members, two distinct cleavage signals with a 2-nt interval could be detected in both degradome data and 5′ RLM-RACE results, suggesting both miR482-type and miR2118-type members can target the *PHAS19* gene (Figure 2b).

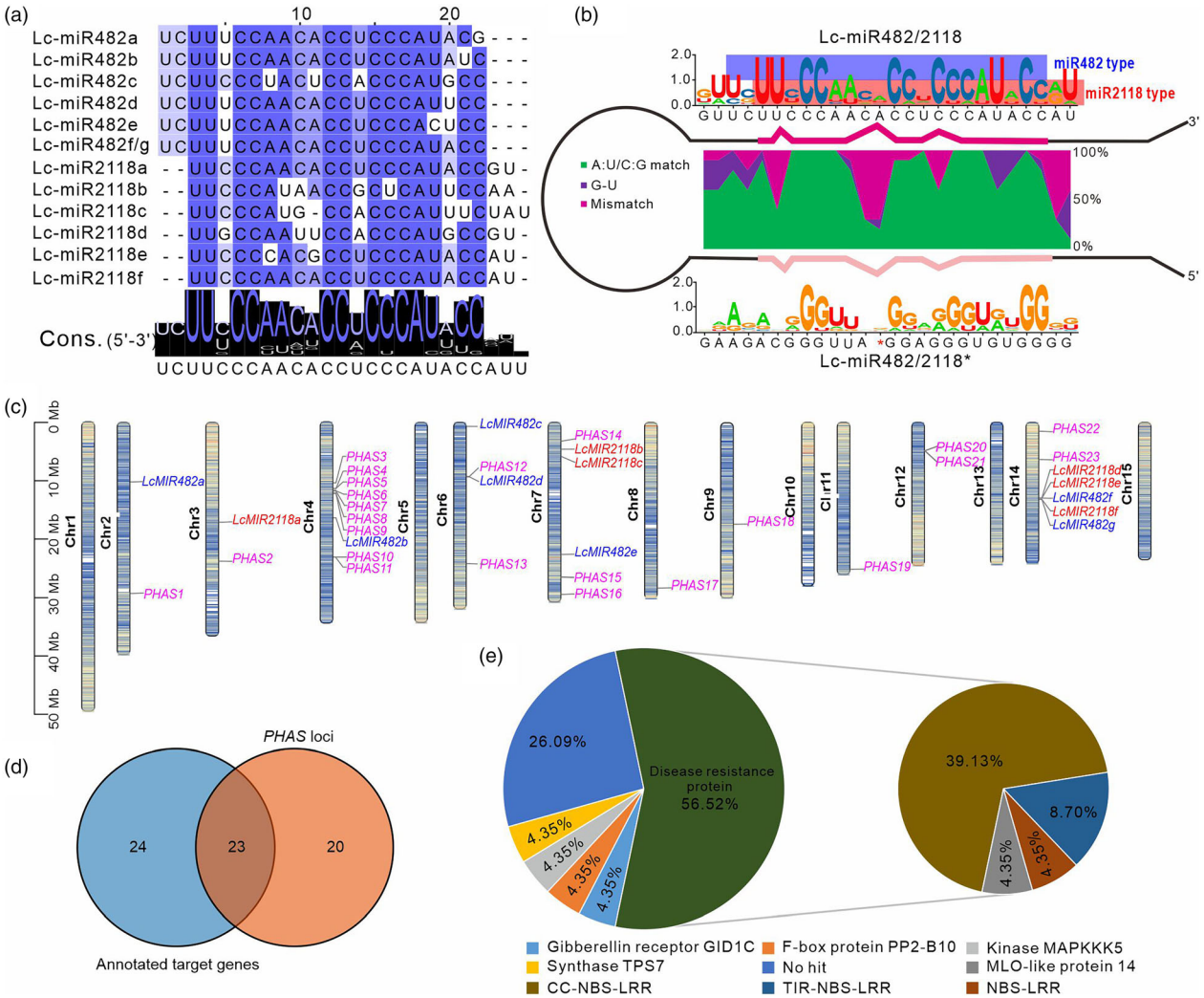

Figure 1 Revisiting of miR482/2118 family and their targets in litchi. (a) Alignment of mature sequences for all litchi miR482/miR2118 family members. (b) Structure and sequence conservation of the miR482/2118 duplex. (c) The distribution of *LcMIR482/2118* and 23 *PHAS* loci targeted by miR482/2118. (d) Venn diagram showed target genes and *PHAS* loci targeted by miR482/2118. (e) Annotation of 23 *PHAS* genes targeted by miR482/2118.

The transcript of *LITCHI007943*, 1306-bp in full-length verified by 5′- and 3′-RACE amplifications, showed a high level of sequence similarity to the GA receptor gene *LcGID1* at the nucleotide level (Figure 2c). However, it can hardly encode a meaningful protein sequence, with the longest open reading frame (ORF) translating into 84 amino acids (Figure 2d) and a low protein-coding potential score evaluated by CPC2 analysis (0.172, http://cpc2.gao-lab.org/), indicating that *LITCHI007943* is likely a long noncoding RNA (lncRNA). The longest predicted ORF region is of a great homology to the GID1 domain (Figure 2d), overlapping with the phasiRNA production region in *LITCHI007943* (Figure 2a,c; Figure S3). We found that these phasiRNAs generated from *LITCHI007943* were able to cleave *LcGID1* homologs in *trans* in litchi (Figure 2e,f; Figures S4 and S5). The gene *LITCHI007943* acted like the *trans*-acting gene (*TAS*) in Arabidopsis, which is noncoding and generates tasiRNAs to regulate downstream genes in *trans*, thus, we named *LITCHI007943* a *TAS-like 1* gene (*LcTASL1*) in litchi. Additionally, *LcTASL1*-derived 21-nt phasiRNAs also acted in *cis* on *LcTASL1*, which likely amplified the silencing effect of Lc-miR482/2118 (Figures S4 and S5).

LcTASL2 enhanced the function of miR482/2118-*LcTASL1* on *LcGID1* via cascade phasiRNA production

In the list of identified *PHAS* loci, we noticed that there was one adjacent to *LcTASL1*, overlapped with an annotated gene *LITCHI007944* (Figure 3a). Sequence analyses revealed that it was also a long noncoding RNA (lncRNA, CPC of 0.197) and possessed great sequence similarity to *LcGID1* and *LcTASL1* (Figure 3b; Figures S6 and S7). In contrast to *LcTASL1*, target site of miR482/2118 was absent in *LITCHI007944* (Figure 3a), suggesting that *LITCHI007944* was not directly targeted by miR482/2118. Its phasiRNA production was likely triggered by phasiRNAs generated from *LcTASL1* because of their high sequence similarity (50.03%) (Figure 3b; Figures S7 and S8). Given the sequence similarity between *LITCHI007944* and *LcGID1* (Figure 3b; Figure S7), phasiRNAs produced from *LITCHI007944* also targeted *LcGID1* in *trans*, similar to *LcTASL1* (Figure S9); therefore, we named *LITCHI007944* as *LcTASL2*. Additionally, both *LcGID1* genes also produced siRNAs without obvious miRNA cleavage signal, mainly from the 2nd exon which possesses great sequence similarity to *LcTASL1* and

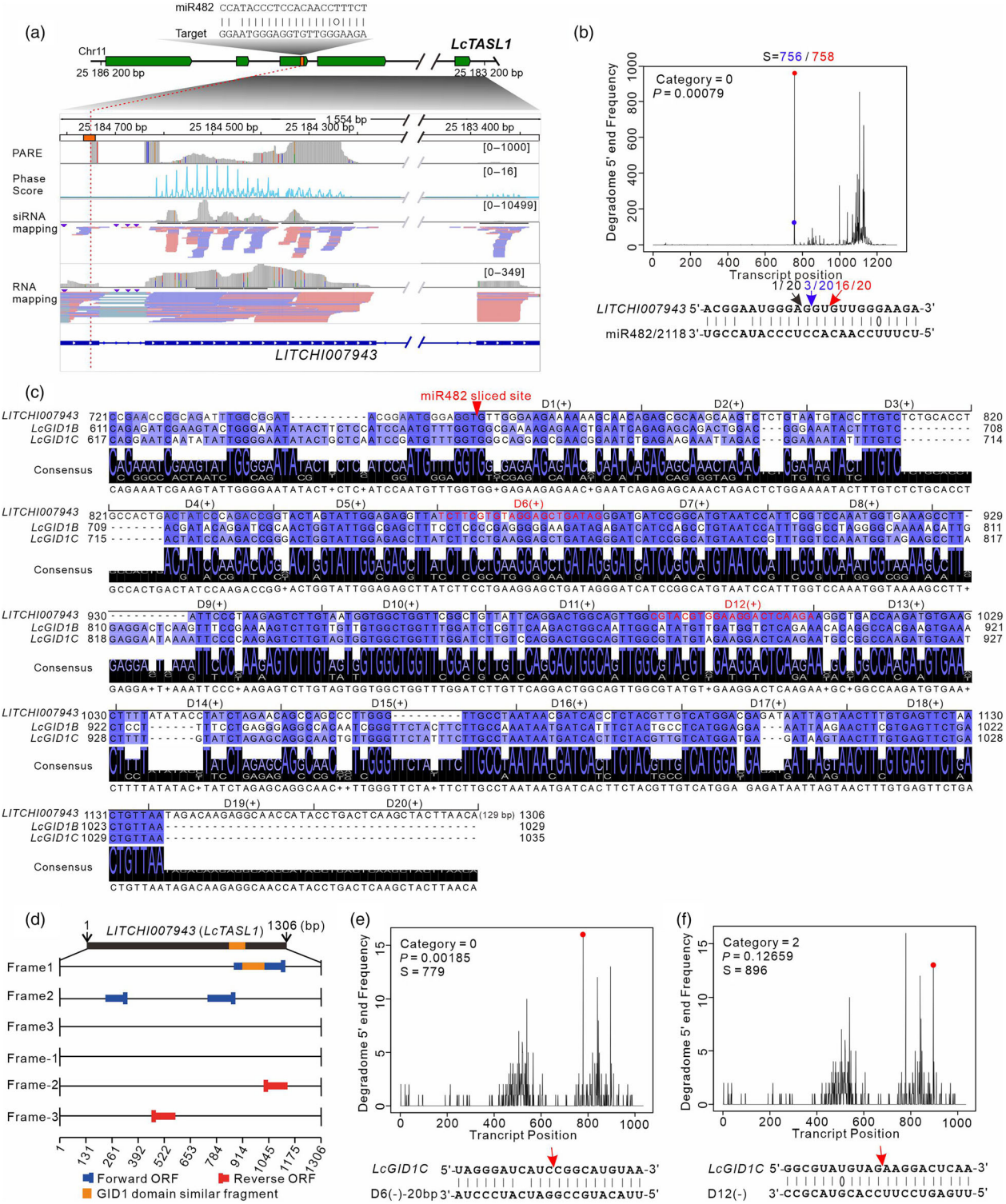

Figure 2 Lc-miR482/2118s target an lncRNA *LcTASL1* ensuing phasiRNA regulating *LcGID1*. (a) miR482/2118 targets *LITCHI007943* leading to the production of abundant phasiRNAs. (b) The miR482/2118-mediated cleavage on *LcTASL1* was validated by both degradome data and 5′ RLM-RACE. Red and blue arrows indicated the cleavage site of the miR482 and miR2118 type member, respectively. Grey arrow indicated others. (c) Sequence similarity shown by alignment of *LITCHI007943* and two *LcGID1* genes. PhasiRNA generated in 21-nt phase beginning with miR482 type member sliced site. (d) *LITCHI007943* is a long noncoding RNA *LcGID1B*. (e) and (f) Represent *LcTASL1*-derived phasiRNA targeted *LcGID1C* validated by degradome sequencing data.

LcTASL2 (Figure 3c,d). Like *LcTASL1*, these phasiRNAs produced from *LcTASL2* and two *LcGID1* genes could act in *cis* on their precursor (Figure S4).

Taken together, we discovered, in litchi, miR482/2118 evolved a new role via targeting a noncoding gene (*LcTASL1*) and generating phasiRNAs to regulate *LcGID1B* and *LcGID1C*,

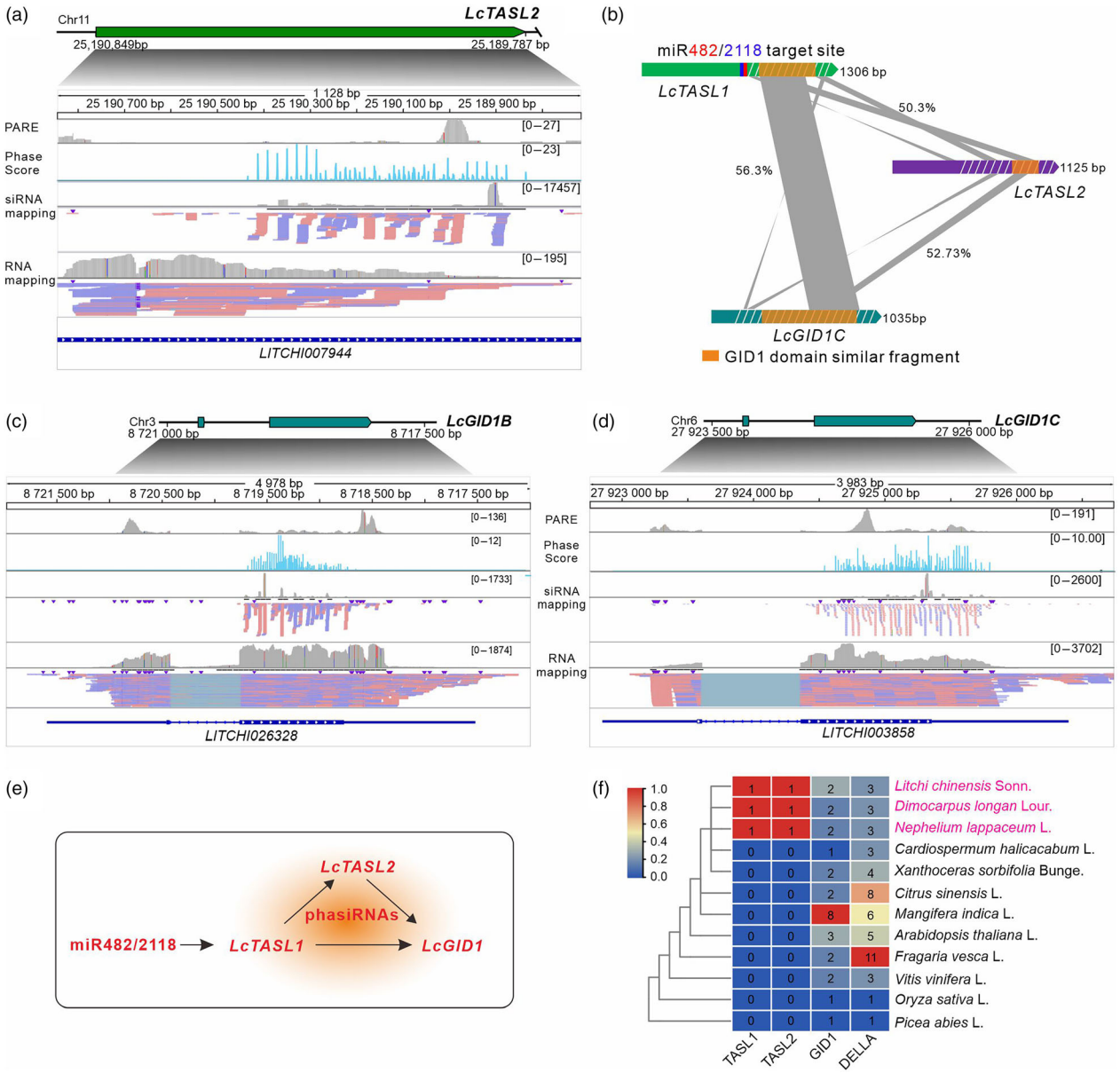

Figure 3 *LcTASL1*-derived phasiRNA triggering phasiRNA production from *LcTASL2* and cascade regulating *LcGID1*. (a) PhasiRNA distribution along *LITCHI007944* (*LcTASL2*). (b) Sequence similarity shown by alignment of two *GID1*-like genes *LcTASL1* and *LcTASL2* with *LcGID1C*. (c, d) PhasiRNA distribution along *LcGID1B* (c) and *LcGID1C* (d). (e) The newly identified pathway of miR482/2118-*TASL-GID1* in litchi. (f) Presentation and absence of *TASL*, *GID1* and *DELLA* homologs in some representative species.

which are involved in GA signalling pathway, meanwhile *LcTASL2* targeted by *LcTASL1*-derived phasiRNAs produce phasiRNAs to reinforce the silencing effects on *LcGID1* genes (Figure 3e). In addition, we also checked the presence/absence of the miR482/2118-*TASL-GID1* pathway in species close to litchi. Comparative analyses revealed that *TASL1* and *TASL2* homologs were present only in certain species from Sapindaceae. Of the five species checked, only three, litchi, longan (*Dimocarpus longan*) and rambutan (*Nephelium lappaceum*), have these two *TASL* genes, and the other two species distant to litchi, balloon-vine (*Cardiospermum halicacabum*) and yellowhorn (*Xanthoceras sorbifolia*) do not have them (Figure 3f), indicating that the miR482/2118-*TASL-GID1* pathway was evolved before the split of the three close species (litchi, longan and rambutan) from the common ancestor (Figure 3f).

The miR482/2118-*TASL-GID1* pathway was likely involved in seed development

To explore the biological function of the newly identified pathway, the expression pattern of *LcTASL1*, *LcTASL2*, *LcGID1* genes and resulting phasiRNAs were analysed in various organs in litchi (Figure S10). PhasiRNAs from these four 21-nt *PHAS* loci were highly enriched in young fruit (Figure S10), as were the expression level of *LcTASL1* and *LcTASL2* (Figure S10). However, *LcGID1B* and *LcGID1C* were relatively lowly expressed in young fruit, but with the highest accumulation in roots (Figure S10). The lower expression of *LcGID1B* and *LcGID1C* in fruit was likely due

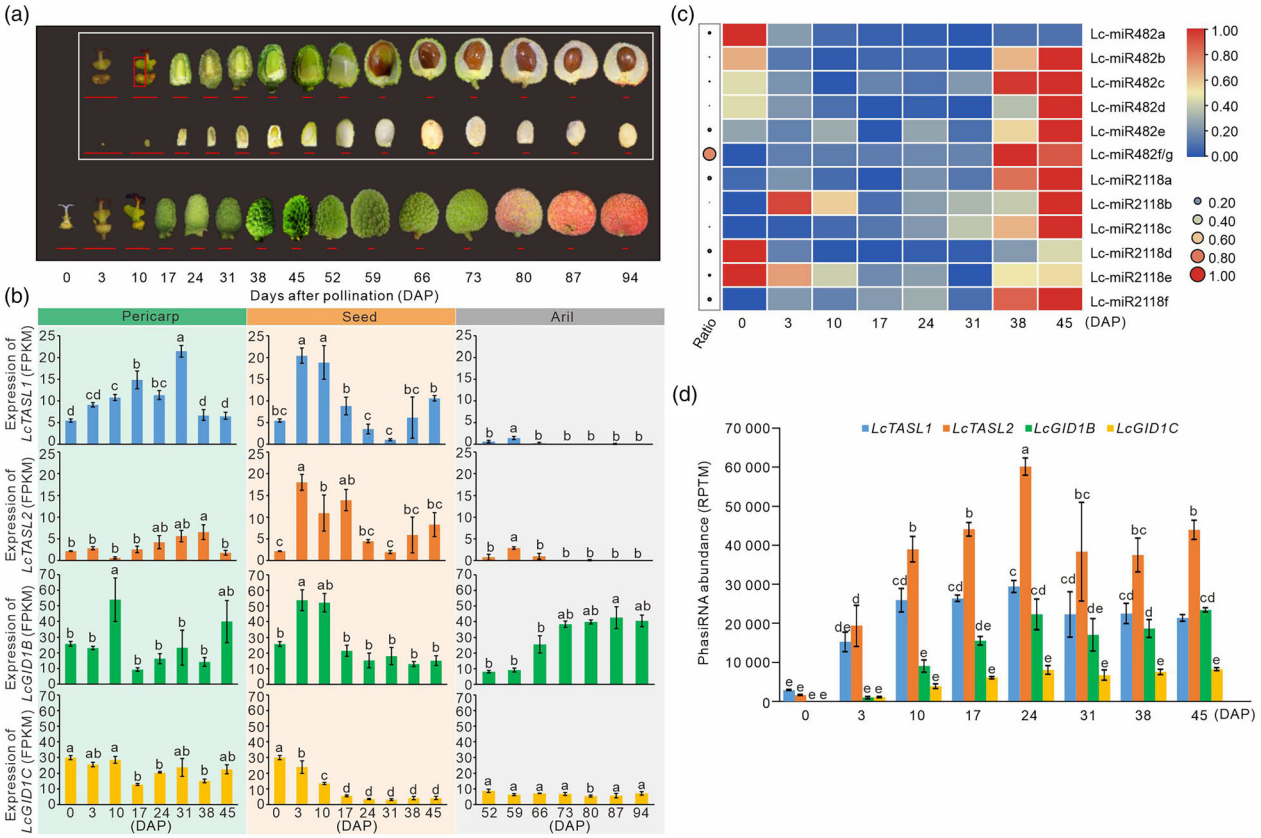

Figure 4 Expression pattern of key genes and associated sRNAs in the miR482/2118-*TASL*-phasiRNA-*GID1* pathway during litchi cv. 'HZ' fruit development. (a) Phenotypes of litchi (cv. 'HZ') fruit development. Samples of 'HZ' fruit were arranged in the black box. Red lines under the fruit samples indicated 0.25 mm. (b) Comparison of the expression levels (Fragments Per Kilobase Million, FPKM) of two *LcTASL* and *LcGID1* genes during 'HZ' fruit development. The green, orange and grey panels indicated the pericarp, seed and aril sampled separated from litchi fruit, respectively. (c) The expression level of miR482/2118s in seed of 'HZ'. (d) The abundance of phasiRNAs (reads per 10 million, RPTM) generated from *LcTASL1*, *LcTASL2*, *LcGID1B* and *LcGID1C* during 'HZ' seed development. Multiple comparisons were conducted within group at different time points. Error bars indicate SEs from three replicates and the letters above bars indicate a significant difference ($P < 0.05$).

to the repressive effect of the phasiRNAs generated from *LcTASL1* and *LcTASL2*. The fruit-preferential expression of *LcTASL1* and *LcTASL2* and the prominent accumulation of phasiRNAs in young fruit suggested that this newly evolved pathway mediated by miR482/2118 might play an important role in litchi fruit development.

To further dissect the detailed function of the pathway in litchi fruit, we collected litchi fruit samples from the cultivar 'Huaizhi' ('HZ') during the whole developmental process from unpollinated ovary to mature fruit (Figure 4a). Transcriptome profiling revealed that *LcTASL1* and *LcTASL2* had higher expression in pericarp and seeds than the aril, in which only low expression was detected in the early stages (Figure 4b), suggesting that these two *LcTASL* genes may be more important in pericarp and seed development. In spite of overall comparable expression levels, *LcTASL1* were of distinct expression trends in pericarp and seed. Its expression increased gradually until reaching the peak level at 31 DAP in pericarp, but it peaked much faster at 3 DAP and decreased slowly in seed (Figure 4b). For *LcTASL2*, it accumulated to a much higher level in seed than in pericarp (Figure 4b). Compared with the two *LcTASL* genes, *LcGID1* genes showed remarkable expression in all tissue samples tested. Overall, the level of *LcGID1B* was higher than *LcGID1C* in all samples (Figure 4c), and both of them showed higher accumulation at early stages of seed development (Figure 4b). All these results suggested that the pathway likely played a more important role in seed than other parts of the litchi fruit.

Next, we checked the expression of sRNA in litchi seed, including both miR482/2118 family and phasiRNAs generated from two *LcTASLs* and *LcGID1s* (Figure 4c,d). We found that most miR482/2118s did not show a consistent expression pattern, agreeing with the diverse function of miR482/2118s. Many of them had higher accumulation at late stages (38–45 DAP, Figure 4c). *LcTASL*/*LcGID1*-derived phasiRNAs were significantly up-regulated after pollination and peaked at 24 DAP, and phasiRNAs derived from *LcTASL2* were of the greatest abundance (Figure 4d), agreeing well with its higher expression level in seed (Figure 4b). This high abundance of phasiRNAs in litchi seed, especially the high accumulation of *LcTASL2*-derived ones, further confirmed the role of this *PHAS* pathway in seed development.

As seed size is a critical phenotypic trait of litchi fruit, fruits with smaller seed are often of greater commercial value. We also profiled the expression of these genes and sRNAs in fruits of 'Nuomici' ('NMC'), a cultivar producing small seed resulted from premature seed abortion (Figure S11). We found that generally the expression of *LcTASLs* and *LcGIDs* in 'NMC' is similar to 'HZ' which produces well-developed large seed. Regarding the downstream phasiRNAs, their accumulation, especially for those

derived from *LcTASL1* and *LcTASL2*, was noticeably accumulated earlier with less abundance in large-seed 'HZ' than aborted-seed 'NMC' (Figure S11). All in all, given the high expression of *LcTASLs* and *LcGID1s* and the profuse accumulation of phasiRNAs in litchi seed, and the important role of GA in plant seed development (Kim *et al*., 2005; Kozaki and Aoyanagi, 2022; Serrani *et al*., 2007), we proposed that the miR482/2118--*TASL-GID1* pathway is likely vital for the seed development in litchi (Huang, 2001; Qiu *et al*., 1994; Ye *et al*., 1992).

Constructed miR482/2118-*TASL-GID1* pathway affected flower and silique development in Arabidopsis

As a perennial fruit tree, litchi lacks a robust transgenic system to valid gene function *in vivo*, therefore, we managed to verify the biological functions of this pathway by constructing miR482/2118-*TASL*-phasiRNA pathway in *Arabidopsis thaliana*, as the GA signalling pathway is conserved between litchi and Arabidopsis. Comparative genomic analyses revealed that there is no homolog of two *LcTASLs* in *Arabidopsis*, while phasiRNA from two *LcTASL* genes could pair well with and target the *GID1* genes of Arabidopsis (Figure 3f; Figures S12 and S13). We firstly performed transformation of single gene of *LcMIR482a*, *LcTASL1* and *LcTASL2*, and then crossed together *LcTASL1* with *LcTASL2* (*LcTASL1* × *LcTASL2*), *LcMIR482a* with *LcTASL1* (*LcTASL1* × *LcMIR482a*) and *LcTASL1* × *LcTASL2* × *LcMIR482a* to examine the effect of *TASL*-derived phasiRNAs on the expression of *AtGID1* genes and the phenotype of transgenic Arabidopsis.

At least three homozygous lines of each transgenic gene were obtained with significantly higher expression than wild type (WT) (Figure S14a–d). Among these homozygous lines, plants with overexpression of *LcTASL1* showed a relatively low expression, which was caused by the cleavage of At-miR472 in Arabidopsis with great sequence similarity to Lc-miR482/2118s (Figures S14c and S15), suggesting that At-miR472-*LcTASL1*-*AtGID1* pathway was built up in the *LcTASL1* transgenic plants. Thus, *LcTASL1*-derived phasiRNA could be triggered by At-miR472 in *LcTASL1* and *LcTASL1* × *LcTASL2* lines, while in *LcTASL1* × *MIR482a* and *LcTASL1* × *LcTASL2* × *LcMIR482a* lines by both At-miR472 and the transformed Lc-miR482a (Figure S14e). In *LcTASL1* × *LcTASL2*, elevated *LcTASL1* caused an increased expression of secondary phasiRNAs (Figure S14e), which significantly reduced the expression of *LcTASL2* (Figure S14d) and *AtGID1* (Figure S14g). Additionally, in *LcMIR482a* × *LcTASL1*, over-accumulated miR482 resulted in the decrease of *LcTASL1* expression (Figure S14c) and then the expression of *AtGID1* (Figure S14g). Compared to *LcTASL1* × *LcTASL2*, introducing the miR482 led to a decrease in the expression of *LcTASL1* (Figure S14c) and *LcTASL2* (Figure S14d) and these phasiRNAs produced from them (Figure S14e,f). All these results showed that phasiRNAs produced by *LcTASL1* could act in *trans* to trigger the production of phasiRNAs from *LcTASL2* and all these *LcTASL1*- and *LcTASL2*-derived phasiRNAs could regulate the *AtGID1s*, which confirmed our proposed regulatory network (Figure 3e).

In these transgenic *Arabidopsis* plants with the build-up of miR482a-*TASL*-phasiRNA pathway, we found that the filament length was significantly reduced in both OX-*LcTASL1* and OX-*LcTASL1* × *LcTASL2* (Figure 5a,b), and the siliques of all transgenic lines containing *LcTASL1* showed different degrees of abnormalities including seed abortion and smaller pod size (Figure 5c–e; Figure S16). The observation that overexpressed *LcTASL1* was negatively associated with the silique length and the ratio of seed number/silique length (Figure 5d,e) suggested the constructed pathway affected seed and fruit development in Arabidopsis. These defects in transgenic lines are quite similar to the phenotype of Arabidopsis *gid1* mutant, which is of shorter filament and shorter siliques with less seeds (Gallego-Giraldo *et al*., 2014; Griffiths *et al*., 2006; Iuchi *et al*., 2007). Thus, these results proved that the miR482/2118-*TASL-GID1* pathway could affect flower and seed formation, and eventually fruit development via the regulation of GA signalling.

GA-responsive factor GAMYB feedback regulates *MIR482/2118*

Our findings have demonstrated that the newly evolved miR482/2118-*TASL-GID1* pathway could regulate litchi seed development via GA signalling. Given the broad regulatory role of GA in fruit development, whether any of these elements in the new regulatory module are under the regulation of GA signalling aroused our curiosity. We then conducted promoter sequence analyses on *LcMIR482/2118s*, *LcTASLs* and *LcGID1s*, and found that a few genes had at least one GA response element (Table S4). The promoters of *LcMIR482d* and *LcMIR482e* contained a GARE-motif, which has been reported to be bound by GA-responsive MYB proteins (GAMYB) that are critical components of GA signalling pathway (Achard *et al*., 2004). Four *GAMYBs* were identified in litchi, in which the expression of *LcGAMYB33* was higher than the other three members in all seed samples, suggesting the importance of LcGAMYB33 (Figure 6a; Figure S17).

To profile the binding target genes of LcGAMYB33, we performed a DNA affinity purification sequencing (DAP-seq) for LcGAMYB33 to unravel its genome-wide binding sites. In total, most (58%) LcGAMYB33 binding peaks were distributed in the genic regions, while 24% was in the intergenic, 11% was in the upstream (<2k from TSS) and only 7% was in the downstream (<2k from TTS) (Figure 6b). A motif with a core sequence of 'TAACTGACT' (e-value = 2.0e-212) was characterized from 70.2% of the LcGAMYB33 binding regions (Figure 6c). For the miR482/2118-*TASL-GID1* module, LcGAMYB33 could bind to the promoter or gene coding regions of *LcMIR482e*, *LcMIR482f*, *LcTASL2*, *LcGID1C* and three *LcDELLA* genes (Figure 6d,e; Figure S18), The *LcMIR482e* has a binding motif of 'AGTTAGTTAG' at around 2 kb before the *MIRNA* precursor region, while the binding motif of 'AAGTTGTTGA' is much closer to the precursor of *LcMIR482f* (Figure 6d,e). These bindings of LcGAMYB33 detected by DAP-seq were further validated by electrophoretic mobility shift assay (EMSA) (Figure 6f,g; Figure S19). The band shift reduced in a competition experiment with increased concentration of unlabelled probes (cold probe) (Figure 6f,g; Figure S19) and mutation of the binding element showed a weak binding band (Figure 6f; Figure S19). We also confirmed the binding ability of another motif 'TCAACAGACT' in *LcMIR482e*, belonging to GARE-motif, which reported to be a binding site of GAMYB (Gubler *et al*., 1999; Figure 6f; Figure S19). To examine whether LcGAMYB33 could regulate *LcMIR482e* and *LcMIR482f*, dual-luciferase reporter assays were performed *in vivo*. A pGreenII 0800 vector containing an LUC reporter gene driven by the *LcMIR482e* and *LcMIR482f* promoter was cotransformed with an empty pGreenII 62-SK vector or pGreenII 62-SK-LcGAMYB33 vector into *N. benthamiana* leaf epidermal cells. Compared with the empty vector samples, the cells expressing *LcMIR482e* and *LcMIR482f* exhibited a significantly higher LUC/REN ratio (Figure 6h). Collectively, these findings support the notion that LcGAMYB33 act as

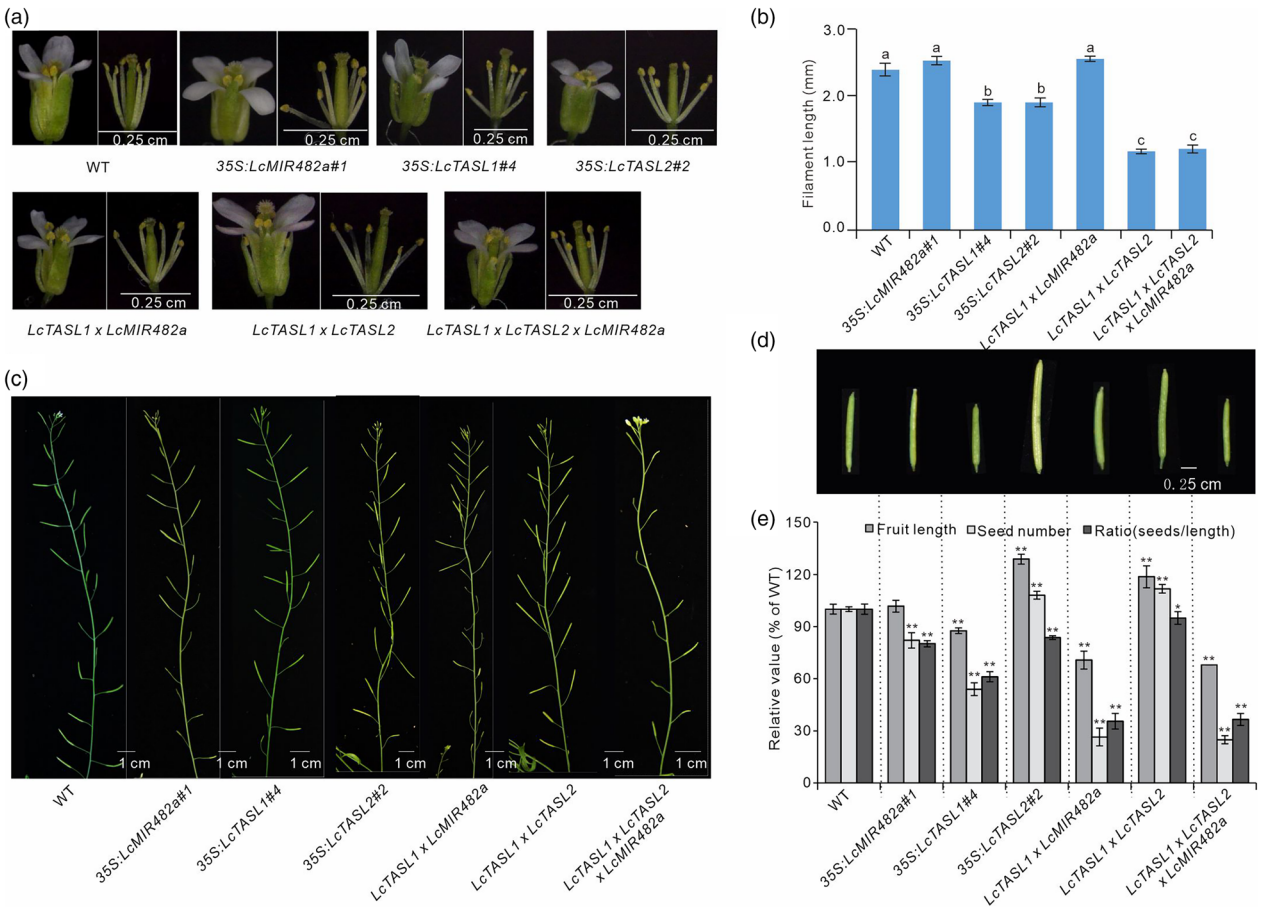

Figure 5 miR482/2118-*TASL-GID1* pathway affected flower and fruit development in *Arabidopsis*. (a) Flower phenotype in different transgenic Arabidopsis lines. (b) Filament length at the eighth node of Arabidopsis plants. Error bar indicated the SE from 10 replicates and each column represented the average value of the length of all filaments of the eighth flowers. Different letters above bars indicate a significant difference ($P < 0.05$) using multiple comparisons. (c) Inflorescence phenotype in different transgenic Arabidopsis lines. (d) Silique phenotype in different transgenic Arabidopsis lines. (e) Maternal phenotype of different Arabidopsis lines compared with wide type (WT) Arabidopsis. Mature fruits were individually harvested and fruit length and seed number were measured. Ratio of seed number to silique length was normalized to the WT. Error bar indicates the SEs from at least five replicates and the asterisk above bar represented the significance level by the Student's *t*-test. Signal asterisk indicated $P < 0.05$, while double asterisk indicated $P < 0.01$.

transcriptional activator of *LcMIR482e* and *LcMIR482f* by directly binding to their promoters. Thus, *LcMIR482e* and *LcMIR482f* were under the transcription regulation of LcGAMYB33, form a new feedback regulatory loop in litchi.

Discussion

In this study, we found that Lc-miR482/2118s gained a novel function by targeting a long noncoding RNA gene, *LcTASL1*, to induce the production of abundant 21-nt phasiRNAs, which negatively regulates the expression of *LcGID1s* to get involved in GA signalling. This silencing effect of *LcTASL1*-derived phasiRNAs can be reinforced by another phasiRNA-generating noncoding RNA gene *LcTASL2* (Figure 7). This pathway of miR482/2118--*TASL-GID* is likely associated with the seed development in litchi. We also found a critical component of the GA signalling, LcGAMYB33, regulated *MIR482/2118* expression at the transcriptional level, functioning as a feedback loop (Figure 7). These results provide the first demonstration of the direct involvement of miRNA in GA signalling via a newly evolved regulatory circuit of phasiRNAs.

Diversification of miR482/2118 functions in litchi

MiR482/2118 superfamily is a 22-nt well-studied miRNA family and widespread in seed plants (Zhang *et al.*, 2021). It originated in gymnosperms and has dual functions in gymnosperms, which was selectively preserved in monocots and eudicots of angiosperms. In eudicots, miR482/2118 mainly targets *NBS-LRRs* to produce phasiRNAs, playing an important role in disease resistance, while in monocots it mainly targets lncRNAs to produce phasiRNAs involved in plant reproductive development (Komiya, 2017; Zhang *et al.*, 2021) In addition to these conserved well-known functions, in our study, based on a new high-quality genome sequence of litchi, in combination with more deep sequencing sRNA data, we have identified more miR482/2118 members and their target genes, suggesting the function of miR482/2118 has expanded greatly in litchi (Hu *et al.*, 2022; Ma *et al.*, 2018). In addition to *NBS-LRRs* and other disease-related genes and the noncoding *LcTASL1* gene of great sequence similarity to the gibberellin receptor *GID1C*, many other target genes have been found in litchi, including those genes homologous to

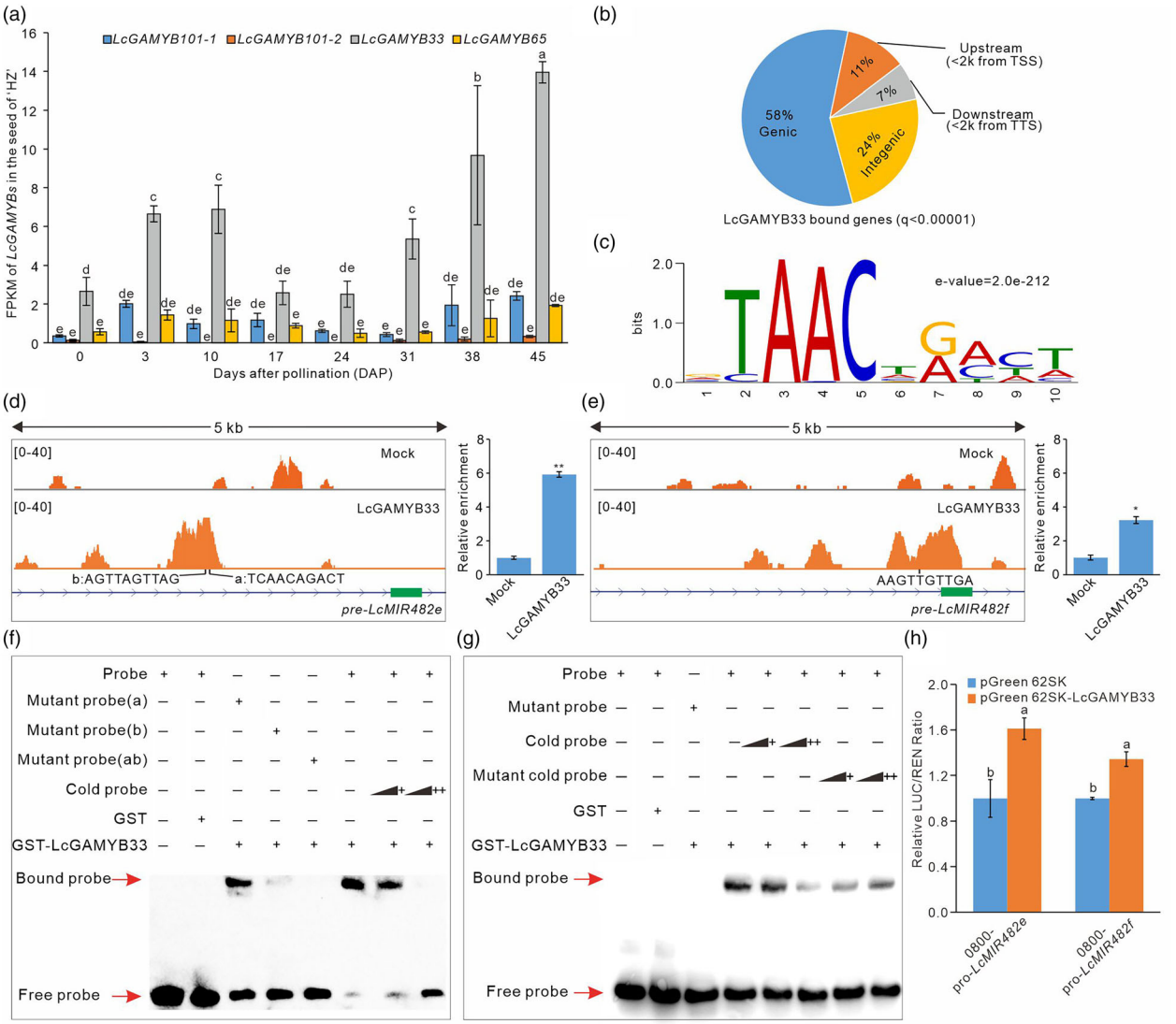

Figure 6 LcGAMYB33 regulated the transcription of *LcMIR482e* and *LcMIR482f*. (a) Expression of four *LcGAMYB* genes in different development stages of 'HZ' seed. Error bars indicate SEs from three biological replicates and different letters above bars indicate a significant difference ($P < 0.05$) using multiple comparisons. (b) Analysis of LcGAMYB33-enriched regions in the DAPseq assay. Pie chart shows the percentage distribution of LcGAMYB33-binding peaks in each category. (c) LcGAMYB33 binding motif identified by DAPseq analysis. (d, e) The binding peaks of LcGAMYB33 in the promoter of *LcMIR482e* (d) and *LcMIR482f* (e). LcGAMYB33 bound *LcMIR482e* via two binding motifs ('a' and 'b'), while just one binding motif showed on *LcMIR482f*. The left panels shown the binding site of LcGAMYB33 on *LcMIR482e* (d) and *LcMIR482f* (e), while the right column indicated the relative enrichment comparing with the empty vector pIX-Halo (Mock). The asterisk above bar represented the significance level by the Student's *t*-test. Signal asterisk indicated $P < 0.05$, while double asterisk indicated $P < 0.01$. (f, g) Electrophoretic mobility shift assays (EMSAs) showing the binding ability of LcGAMYB33 with the promoters of *LcMIR482e* (f) and *LcMIR482f* (g) *in vitro*. The shifted bands indicated by arrows suggest the formation of DNA–protein complexes. '+' and '−' represent presence and absence, respectively. Triangles indicate increasing amounts of mutant or unlabelled probes used for testing the specificity of binding and competition. Probes without biotin labels were loaded as unlabelled competitors. GST protein alone was used as the negative control. In f, 'Mutant probe (a)' and 'Mutant probe (b)' signify the sequence mutation of motif a and b, respectively, while 'mutant (ab) probe' denotes the mutations made in both binding motifs simultaneously. (h) LcGAMYB33 activated the expression of *LcMIR482e* and *LcMIR482f in vivo*, as shown by transient dual-luciferase reporter assays. Both effector and reporter vectors were cotransformed into tobacco leaves. After incubation of 72 h, the ratio of LUC to REN was detected. Error bars indicate SEs from six replicates. Different letters indicate a significant difference ($P < 0.05$) using multiple comparisons.

BR-signalling kinase 1 (BSK1), calcium-transporting ATPase, SUPPRESSOR OF GENE SILENCING 3 protein, etc. (Table S3). These genes are involved in different biological processes, for instance, BSK1 acts as a positive regulator of brassinosteroid (BR) signalling (Wang and Chory, 2006). Similar to *LcTASL1* of miR482/2118, other target genes might be lineage- or species-specific, i.e., most of these target genes are newly evolved. These results provide a great demonstration that miR482/2118 is in a process of rapid gaining and losing of specific target genes in plants, in addition to its conserved function in disease resistance. Its more diverse function renders miR482/2118 great capacity to participate in more regulatory network of complex trait development, for instance, the seed development in litchi.

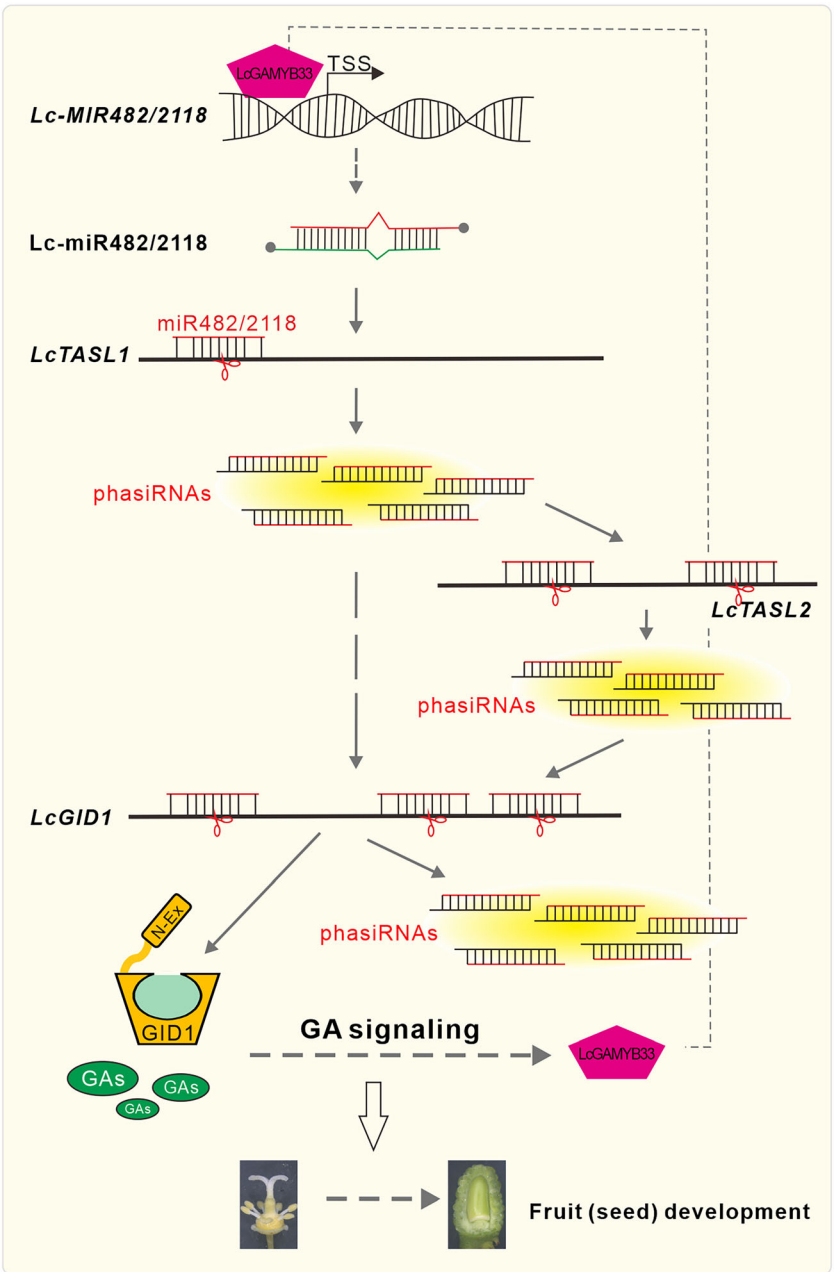

Figure 7 Perspective model of the miR482/2118-*TASL-GID1* regulatory pathway. Lc-miR482/2118s targets a species-specific noncoding gene *LcTASL1* and triggers the generation of secondary phasiRNAs to regulate in *trans* the expression of GA receptor gene *LcGID1*; this silencing effect on *LcGID1* is reinforced by phasiRNAs from another noncoding *PHAS* gene *LcTASL2*. This pathway is associated with the fruit development of litchi via the involvement in GA signalling. Lc-miR482/2118s is under the transcriptional regulation of LcGAMYB33, a critical component of GA signalling, forming a feedback regulatory loop.

Crosstalk between miR482/2118s and gibberellin signalling via secondary and tertiary phasiRNAs in plants

PhasiRNAs, a major class of siRNA, are generally induced by 22-nt miRNA to regulate plant development and environmental adaption (Liu *et al*., 2020). It could not only act in *cis* to cleave their precursors to enhance the silencing effect of miRNAs, but also function in *trans* to regulate genes other than the parental genes to further expand the functions of miRNAs (Liu *et al*., 2020; Tamim *et al*., 2018). Zhang *et al*. (2020) and Jiang *et al*. (2020) proved that in rice these 21-nt phasiRNAs generated from miR2118 *PHAS* loci acted in a target-cleavage mode to regulate a large variety of genes, eventually affecting rice sterility, suggesting phasiRNAs expanding the functions of miR2118 family. In addition, several studies have found that secondary siRNAs can induce tertiary phasiRNA production. For example, in eudicots, At-miR173 and other related miRNAs belonging to the super-miR7122 family regulate a set of *pentatricopeptide repeat (PPR)* genes via one or two layers of noncoding *trans*-acting like genes (*TASL*), and secondary and tertiary phasiRNAs were generated to act in *cis* or in *trans* (Xia *et al*., 2013).

In this study, we have confirmed that an lncRNA target *LcTASL1* of miR482/2118 via cascade 21-nt phasiRNAs to repress the expression of the gibberellin receptor *GID1* genes, suggesting miR482/2118 is directly involved in gibberellin signalling. Firstly, secondary 21-nt phasiRNAs generated from *LcTASL1* by miR482/2118 can directly target and cleave *LcGID1* and *LcTASL2* mRNA (Figure 2e,f; Figures S5 and S8), and tertiary 21-nt phasiRNAs from *LcTASL2* and *LcGID1s* themselves can enhance the silence effect on *LcGID1* genes (Figures S4 and S9). Meanwhile, several 22-nt siRNA produced from *LcTASL* and *LcGID1* also might contribute to this pathway for its relatively high proportion

(Figure S20). For example, a 22-nt phasiRNA (sequence: 5′ UUGAGUCCUUCCACGUACGCCA 3′) generated from *LcTASL1* had a significant cleavage signal on *LcTASL2* (Figure S20b). GID1 perception is the first step of GA response, and GA is a critical hormone in modulating diverse plant developmental processes including seed germination, flower development, fruit initiation and seed development, suggesting miR482/2118-*TASL-GID1* pathway might participate in multiple biological processes in litchi. These two *LcTASL* genes were characterized only in litchi, longan (*D. longan*) and rambutan (*N. lappaceum*), all of which are important subtropical and tropical economic fruit trees belonging to the Nepheliinae subtribe of Sapindaceae (Figure 3f), indicating that the miR482/2118-*TASL-GID1* pathway was evolved from a common ancestor of the three close species (litchi, longan and rambutan). Thus, it is reasonable to believe that the miR482/2118-*TASL-GID1* pathway may be associated with the development of certain traits unique to them, for instance, the formation of freshy aril.

MiR482/2118 regulate the seed development via GA signalling

Recently, it was reported that miR482/2118, in addition to the targeting of *NBS-LRRs* in disease resistance, can induce the production of 21-nt reproductive phasiRNAs, which were enriched in pre-meiotic stages of anther, in a few eudicots such as flax, strawberry and columbine (Pokhrel *et al*., 2021; Zhang *et al*., 2021). Similar to the reproductive phasiRNAs in monocots, these 21-nt phasiRNAs likely play a crucial role in male reproductive development (Pokhrel *et al*., 2021). However, how they are involved in plant reproductive development still remains largely unknown. Increasing studies conducted in monocots, especially in rice, found that 21-nt reproductive phasiRNAs function via targeting a large number of functional genes to reprogram the mRNA transcriptome in early stage of anther development (Araki *et al*., 2020; Fan *et al*., 2016; Jiang *et al*., 2020; Lan *et al*., 2022; Zhang *et al*., 2020). Overall, these studies mainly focused on the male part, the anther development. In this study, we found miR482/2118 also participated in plant reproduction, but it is irrelevant to the flower organ, instead, it regulates the fruit development, especially the seed development, via the *LcTASL-LcGID1* cascade and subsequent GA signalling. On the other hand, with in-depth and broad sRNA profiling, we were not able to detect the type of reproductive phasiRNA found in other eudicots (Pokhrel *et al*., 2021) from litchi anther, suggested that the miR482/2118-directed reproductive phasiRNAs are probably dynamically evolved, as the miR2275-type 24-nt reproductive phasiRNAs reported in eudicots (Xia *et al*., 2019). Apart from the role in fruit development, miR482/2118 may serve many other roles which are promising for further investigation, given the importance of the hormone GA in plant growth and development. The feedback regulation of GAMYB on the transcription of *MIR482/2118* suggested a complicated crosstalk between the miR482/2118-mediated gene silencing and the GA signalling network.

Methods

Plant materials

Litchi samples including *L. chinensis* Sonn. cv. 'Huaizhi' ('HZ') and 'Nuomici' ('NMC') were grown in an orchard located at South China Agricultural University (Guangzhou, China). Three litchi trees with consistent growth potential were selected as three biological replicates. Fruits were collected from different branches of each tree. When possible, fruit of 'HZ' and 'NMC' were dissected into different tissues including ovary, seed, pericarp and aril before freezing.

Construction and cultivation of transgenic lines

Overexpression vectors of 35S: *LcTASL1*, 35S: *LcTASL2* and 35S: *LcMIR482a* were generated by cloning the full length of *LcTASL1*, *LcTASL2* and precursor sequence of *Lc-MIR482a* into the vector pCAMBIA1302. The precursor sequence of *LcMIR482a* was amplified including the stem loop and its upstream and downstream 200 bp. The above plasmids were transformed into *A. thaliana* (L.) ecotype Columbia-0 (Col-0) plants via *Agrobacterium tumefaciens*-mediated stable transformation based on the floral dip transformation method (Zhang *et al*., 2006). At least three homozygous lines carrying the overexpression transgene of 35S: *LcTASL1* were chosen to cross with the other two transgenic lines (35S: *LcTASL2* and 35S: *LcMIR482a*). The result hybrid offspring, including 35S: *LcTASL1#4* × 35S: *LcTASL2#2* (*LcTASL1* × *LcTASL2*), 35S: *LcTASL1#4* × 35S: *LcMIR482a#1* (*LcTASL1* × *LcMIR482a*) and 35S: *LcTASL1#4* × 35S: *LcTASL2#2* × 35S: *LcMIR482a#1* (*LcTASL1* × *LcTASL2* × *LcMIR482a*) were used for phenotype and functional analyses. WT and transgenic *Arabidopsis* plants were grown in a greenhouse, and the growth conditions were 22 °C (day)/19 °C (night) in long days (16 h light/8 h dark).

All experimental samples for the assays were arranged completely at random. There were at least six replicates of each type of Arabidopsis sample for phenotypic measurements. The silique length and seed number present at the eighth node of the principal Arabidopsis inflorescence were quantitatively assessed. The results were expressed as mean ± standard error and $P < 0.05$ was set as the minimum significant difference by the Student's *t*-test.

Rapid-amplification of cDNA ends (RACE)

To acquire the full-length cDNA sequence of *LcTASL1* and *LcTASL2*, we performed 5′-RACE and 3′-RACE experiments following the manufacturer's instructions accompanying the SMARTer® RACE 5′/3′ kit (TAKARA). To map the cleavage sites in the *LcTASL1* transcript, we performed modified 5′-RNA ligase-mediated rapid amplification of cDNA ends (5′-RLM-RACE) mainly following the method of Shahid *et al*. (2018). The cDNA templates were amplified through two rounds of PCR with the universal sense or antisense primers and two gene-specific primers (Table S5). The PCR products were cloned into the pEASY vector (pEASY®-Blunt Cloning Kit, TransGen Biotech) and then sequenced in Sangon Biotech (Shanghai). Primers used in 5′ and 3′ RACE were provided in Table S5.

Phylogenetic analysis

For phylogenetic analysis, the genome and amino acid sequence of all species used in this study were obtained from Phytozome (https://phytozome-next.jgi.doe.gov/) and Sapbase (Li *et al*., 2022). Full length of *LcTASL1* and *LcTASL2* were used to blast to other genome sequences by TBtools (Chen *et al*., 2020) to identify homolog genes. Similarly, GID1 homologs were determined by homolog search as well. Finally, a species tree was constructed using the selected species and the number of homologous genes identified in each species was displayed in heatmap by TBtools (Chen *et al*., 2020).

qRT-PCR analysis

Quantitative reverse transcription–polymerase chain reaction (qRT-PCR) was conducted with Promega GoTaq® qPCR Master Mix (A6001) in a BioRad CFX384 Real-Time PCR Detection System, with three biological replicates and three technical replicates. The *LcGAPDH* and *LcEF1α* were used for litchi mRNA sample control, and the *AtACT* and *AtU6* were used as Arabidopsis miRNA sample control, respectively. The relative expression was calculated using the comparative $2^{(-\Delta\Delta C_T)}$ method (Pfaff, 2001). Details regarding the qPCR primers were provided in Table S5.

RNA-Seq and data analysis

Total RNA was extracted using PureLink™ Plant RNA purification Reagent (Invertrogen, Code No: 12322012) from ovary, seed and pericarp, while the aril RNA was extracted using a hot-boron-based method (Kong *et al*., 2022); 1 μg high-quality RNA from 132 samples with high quality was sent to BioMaker (China, Beijing) for mRNA library construction and RNA sequencing (RNA-seq). In total, 132 mRNA libraries were constructed and sequenced on a NovaSeq 6000 platform.

Quality control of raw data was conducted using FastQC (Andrews, 2010) and MultipleQC (Ewels *et al*., 2016) to confirm acceptable quality for downstream analysis. Fastp software (S. Chen *et al*., 2018) was invoked to remove the low-quality bases present in the sequencing data at the 3′ end of the splice sequence and read segment. All sequence data were compared to the reference genome of litchi using STAR software (Dobin *et al*., 2013). The expression of litchi genes was calculated using StringTie software (Pertea *et al*., 2015).

sRNA-seq and data analysis

Two -microgram total RNA of each sample was sent to Novogene (Beijing, China) for sRNA library construction and sequencing (sRNA-seq). In total, 48 sRNA libraries were constructed and sequenced on an Illumina HiSeq 2000 platform. All sRNA data, including those from the previous study of Ma *et al*. (2018) were analysed according to our previous published methods (Chen *et al*., 2021; Feng *et al*., 2019).

DAP-seq and data processing

The DNA affinity purification sequencing (DAP-seq) experiment was performed mainly according to the previously published protocol (Bartlett *et al*., 2017; O'Malley *et al*., 2016). Briefly, 5 μg genomic DNA was extracted from young leaves of 'FZX', the litchi cultivar with genome sequenced and normally developing aborted seed (Figure S21) and fragmented into 200-bp fragments by ultrasonication. The fragments were ligated with Illumina-based sequencing adaptors to form a DNA library. The *LcGAMYB33* coding sequence was cloned into pIX-Halo vector and translated *in vitro* using TNT® SP6 High-Yield Wheat Germ Protein Expression System (L3260) from Promega Corporation. After incubation of a litchi genome DNA library with HALO-tagged LcGAMYB33, DNA complex (a DNA-protein complex) was eluted to amplify with indexed primer and then sequenced in Novogene (Beijing, China). Quality control of raw data was processed by FastQC (Andrews, 2010). Clean reads were aligned against litchi reference genome by bowtie2 (Langmead and Salzberg, 2012) and converted into visual files that can be viewed on IGV by Samtools (Li *et al*., 2009). Peaks calling was performed by Macs2 (Gaspar, 2018) and MEME-ChIP suite was used to discover binding motifs (Machanick and Bailey, 2011).

Electrophoretic mobility shift assay

The partial sequence of *LcGAMYB33* containing the DNA binding domain was cloned into the pGEX4T-GST vector harbouring a GST tag (Table S5). The resulting plasmid was transformed into *Escherichia coli* BL21 (DE3) (Tsingke Biotechnology Company, Beijing, China) for the production of recombinant GST-LcGAMYB33. GST-LcGAMYB33 was purified by GSTPur Glutathione Kit (SA008K; Smart-Lifesciences, Changzhou, Jiangsu Province, China) following kit protocol. Protein concentrations were determined using a Nano Drop 2000 spectrophotometer (Thermo Scientific). Electrophoretic mobility shift assays (EMSAs) were performed following the manufacturer's instructions of LightShift® Chemiluminescent EMSA Kit (Thermo Fisher Scientific, 20148). Briefly, biotin-labelled probes and GST-LcGAMYB33 were incubated together, while unlabelled and mutated probes and GST protein alone were used as competitors and negative controls, respectively. Thereafter, free and protein–DNA complexes were separated on a 5% native polyacrylamide gel, transferred onto nylonmembrane and detected by a chemiluminescent imaging system (Beijing kcrx bio-company, K 3000mini).

Dual-luciferase reporter assays

The promoter fragments (1500 bp) of *LcMIR482e* and *LcMIR482f* were constructed in the pGreenII 0800-LUC to generate reporter constructs, and *LcGAMYB33* gene was inserted into the empty pGreenII 62-SK vector as the effectors. Both effector and reporter constructs were individually introduced into *A. tumefaciens* GV3101 (pSoup), and the bacteria were injected into tobacco (*Nicotiana benthamiana*) leaves with needleless syringes for transient expression assays. For coinjection with effector and reporter constructs, the bacteria were resuspended in infiltration buffer (10 mM MES, 10 mM $MgCl_2$, 150 μM acetosyringone, pH 5.6) at OD_{600} = 0.65 and incubated for 3 h at room temperature. The leaf zones of infiltration were harvested for enzyme activities assays of firefly luciferase and renilla luciferase at 3-day postinjection using the DualLuciferase® Reporter Assay System (YEASEN, Shanghai, China). At least six independent biological replicates were examined. Details regarding the Dual-luciferase reporter assays primers were provided in Table S5.

Acknowledgements

This study was funded by the Guangdong Laboratory of Lingnan Modern Agriculture (Project: NZ2021007). This work was supported by the National Natural Science Foundation of China (#32072547, #31872063). The Special Support Program of Guangdong Province (Grant No. 2019TX05N193). We thank members of the Xia and Li labs for helpful discussions.

Author contributions

R. Xia and Y. Zhang designed and conducted this study. Y. Zhang performed the experiments with the help of Z. Zeng, H. Hu, M. Zhao, X. Ma, Y. Liu, Y. Hao and J. Xu, while analysed the data with the assistance of C. Chen and G. Li, Y. Zhang and R. Xia wrote the paper.

Conflict of interest

The authors declare no conflict of interest.

Data availability

The sRNA and PARE data sets generated from Ma *et al*. (2018) study have been deposited in National Center for Biotechnology Information (NCBI) Gene Expression Omnibus (GEO) under the accession number GSE98698. All RNA-seq and sRNA-seq data generated from this study were deposited in NCBI under the BioProject ID number PRJNA951495.

References

Achard, P., Herr, A., Baulcombe, D.C. and Harberd, N.P. (2004) Modulation of floral development by a gibberellin-regulated microRNA. *Development*, **131**, 3357–3365.

Achkar, N.P., Cambiagno, D.A. and Manavella, P.A. (2016) miRNA biogenesis: a dynamic pathway. *Trends Plant Sci.* **21**, 1034–1044.

Allen, E., Xie, Z., Gustafson, A.M. and Carrington, J.C. (2005) microRNA-directed phasing during *trans*-acting siRNA biogenesis in plants. *Cell*, **121**, 207–221.

Andrews, S. (2010) *FastQC: a quality control tool for high throughput sequence data. Babraham Inst*. http://www.bioinformatics.babraham

Araki, S., Le, N.T., Koizumi, K., Villar-Briones, A., Nonomura, K.I., Endo, M., Inoue, H. *et al*. (2020) miR2118-dependent U-rich phasiRNA production in rice anther wall development. *Nat. Commun.* **11**, 3115.

Arnaud, N., Girin, T., Sorefan, K., Fuentes, S., Wood, T.A., Lawrenson, T. *et al*. (2010) Gibberellins control fruit patterning in *Arabidopsis thaliana*. *Genes Dev.* **24**, 2127–2132.

Axtell, M.J. (2013) Classification and comparison of small RNAs from plants. *Annu. Rev. Plant Biol.* **64**, 137–159.

Bartlett, A., O'Malley, R.C., Huang, S.S.C., Galli, M., Nery, J.R., Gallavotti, A. and Ecker, J.R. (2017) Mapping genome-wide transcription-factor binding sites using DAP-seq. *Nat. Protoc.* **12**, 1659–1672.

Borges, F. and Martienssen, R.A. (2015) The expanding world of small RNAs in plants. *Nat. Rev. Mol. Cell Biol.* **16**, 727–741.

Canto-pastor, A., Santos, B.A.M.C., Valli, A.A., Summers, W., Schornack, S. and Baulcombe, D.C. (2019) Enhanced resistance to bacterial and oomycete pathogens by short tandem target mimic RNAs in tomato. *Proc. Natl Acad. Sci. USA*, **116**, 2755–2760.

Chen, C., Zeng, Z., Liu, Z. and Xia, R. (2018) Small RNAs, emerging regulators critical for the development of horticultural traits. *Hortic. Res.* **5**, 6–8.

Chen, S., Zhou, Y., Chen, Y. and Gu, J. (2018) Fastp: an ultra-fast all-in-one FASTQ preprocessor. *Bioinformatics*, **34**, i884–i890.

Chen, C., Chen, H., Zhang, Y., Thomas, H.R., Frank, M.H., He, Y. and Xia, R. (2020) TBtools: an integrative toolkit developed for interactive analyses of big biological data. *Mol. Plant*, **13**, 1194–1202.

Chen, C., Li, J., Feng, J., Liu, B., Feng, L., Yu, X., Li, G. *et al*. (2021) sRNAanno – a database repository of uniformly annotated small RNAs in plants. *Hortic. Res.* **8**, 45.

Dobin, A., Davis, C.A., Schlesinger, F., Drenkow, J., Zaleski, C., Jha, S. *et al*. (2013) STAR: ultrafast universal RNA-seq aligner. *Bioinformatics*, **29**, 15–21.

Ewels, P., Magnusson, M., Lundin, S. and Käller, M. (2016) MultiQC: summarize analysis results for multiple tools and samples in a single report. *Bioinformatics*, **32**, 3047–3048.

Fan, Y., Yang, J., Mathioni, S.M., Yu, J., Shen, J., Yang, X. *et al*. (2016) *PMS1T*, producing phased small-interfering RNAs, regulates photoperiod-sensitive male sterility in rice. *Proc. Natl Acad. Sci. USA*, **113**, 15144–15149.

Feng, L., Xia, R. and Liu, Y. (2019) Comprehensive characterization of miRNA and *PHAS* loci in the Diploid Strawberry (*Fragaria vesca*) genome. *Hortic. Plant J.* **5**, 255–267.

Gallego-Giraldo, C., Hu, J., Urbez, C., Gomez, M.D., Sun, T. and Perez-Amador, M.A. (2014) Role of the gibberellin receptors GID1 during fruit-set in Arabidopsis. *Plant J.* **76**, 1020–1032.

Gao, S. and Chu, C. (2020) Gibberellin metabolism and signaling: Targets for improving agronomic performance of crops. *Plant Cell Physiol.* **61**, 1902–1911.

Gaspar, J.M. (2018) *Improved peak-calling with MACS2. bioRxiv*. https://doi.org/10.1101/496521

Griffiths, J., Murase, K., Rieu, I., Zentella, R., Zhang, Z.-L., Powers, S.J. *et al*. (2006) Genetic characterization and functional analysis of the GID1 gibberellin receptors in *Arabidopsis*. *Plant Cell*, **18**, 3399–3414.

Gubler, F., Raventos, D., Keys, M., Watts, R., Mundy, J. and Jacobsen, J.V. (1999) Target genes and regulatory domains of the GAMYB transcriptional activator in cereal aleurone. *Plant J.* **17**, 1–9.

Hu, G., Feng, J., Xiang, X., Wang, J., Salojärvi, J., Liu, C., Wu, Z. *et al*. (2022) Two divergent haplotypes from a highly heterozygous lychee genome suggest independent domestication events for early and late-maturing cultivars. *Nat. Genet.* **54**, 73–83.

Huang, H. (2001) Towards a better insight into the development of the arillate fruit of litchi and longan. *Acta Hortic.* **558**, 185–192.

Iuchi, S., Suzuki, H., Kim, Y.C., Iuchi, A., Kuromori, T., Ueguchi-Tanaka, M. *et al*. (2007) Multiple loss-of-function of Arabidopsis gibberellin receptor AtGID1s completely shuts down a gibberellin signal. *Plant J.* **50**, 958–966.

Jiang, P., Lian, B., Liu, C., Fu, Z., Shen, Y., Cheng, Z. and Qi, Y. (2020) 21-nt phasiRNAs direct target mRNA cleavage in rice male germ cells. *Nat. Commun.* **11**, 5191.

Kim, Y.C., Nakajima, M., Nakayama, A. and Yamaguchi, I. (2005) Contribution of gibberellins to the formation of *Arabidopsis* seed coat through starch degradation. *Plant Cell Physiol.* **46**, 1317–1325.

Komiya, R. (2017) Biogenesis of diverse plant phasiRNAs involves an miRNA-trigger and Dicer-processing. *J. Plant Res.* **130**, 17–23.

Kong, X., Zeng, J., Yun, Z., Hu, C., Yang, B., Qu, H., Jiang, Y. *et al*. (2022) Characterization of miRNA-mediated auxin signaling during banana (*Musa* spp.) fruit ripening. *Postharvest Biol. Technol.* **193**, 112045.

Kozaki, A. and Aoyanagi, T. (2022) Molecular aspects of seed development controlled by gibberellins and abscisic acids. *Int. J. Mol. Sci.* **23**, 1876.

Lan, T., Yang, X., Chen, J., Tian, P., Shi, L., Yu, Y. *et al*. (2022) Mechanism for the genomic and functional evolution of the MIR2118 family in the grass lineage. *New Phytol.* **233**, 1915–1930.

Langmead, B. and Salzberg, S.L. (2012) Fast gapped-read alignment with Bowtie 2. *Nat. Methods*, **9**, 357–359.

Li, H., Handsaker, B., Wysoker, A., Fennell, T., Ruan, J., Homer, N. *et al*. (2009) The sequence alignment/map format and SAMtools. *Bioinformatics*, **25**, 2078–2079.

Li, J., Chen, C., Zeng, Z., Wu, F., Feng, J., Liu, B., Mai, Y. *et al*. (2022) *SapBase (Sapinaceae Genomic DataBase): a central portal for functional and comparative genomics of Sapindaceae species. bioRxiv*. https://doi.org/10.1101/2022.11.25.517904

Liu, Y., Teng, C., Xia, R. and Meyers, B.C. (2020) Phased secondary small interfering RNAs (phasiRNAs) in plants: their biogenesis, genic sources, and roles in stress responses, development, and reproduction. *Plant Cell*, **32**, 3059–3080.

Ma, W., Chen, C., Liu, Y., Zeng, M., Meyers, B.C., Li, J. and Xia, R. (2018) Coupling of microRNA-directed phased small interfering RNA generation from long noncoding genes with alternative splicing and alternative polyadenylation in small RNA-mediated gene silencing. *New Phytol.* **217**, 1535–1550.

Machanick, P. and Bailey, T.L. (2011) MEME-ChIP: Motif analysis of large DNA datasets. *Bioinformatics*, **27**, 1696–1697.

O'Malley, R.C., Huang, S.S.C., Song, L., Lewsey, M.G., Bartlett, A., Nery, J.R. *et al*. (2016) Cistrome and epicistrome features shape the regulatory DNA landscape. *Cell*, **165**, 1280–1292.

Pertea, M., Pertea, G.M., Antonescu, C.M., Chang, T.-C., Mendell, J.T. and Salzberg, S.L. (2015) StringTie enables improved reconstruction of a transcriptome from RNA-seq reads. *Nat. Biotechnol.* **33**, 290–295.

Pfaff, W.M. (2001) A new mathematical model for relative quantification in real-time RT–PCR. *Nucleic Acids Res.* **29**, 2003–2007.

Pokhrel, S., Huang, K., Bélanger, S., Zhan, J., Caplan, J.L., Kramer, E.M. and Meyers, B.C. (2021) Pre-meiotic 21-nucleotide reproductive phasiRNAs emerged in seed plants and diversified in flowering plants. *Nat. Commun.* **12**, 4941.

Qiu, Y., Zhang, Z. and Qiu, R. (1994) Study on embryo and endosperm development of *Litchi Chinensis* sonn. *Chin. Bull. Bot.* **11**, 45–47.

Qiu, Y., Xiang, X., Wang, B., Zhang, Z. and Yuan, P. (1998) Endogenous hormone balance in three types of litchi fruit and their fruit set mechanism. *Fruit Sci.* **15**, 39–43.

Serrani, J.C., Fos, M., Atarés, A. and García-Martínez, J.L. (2007) Effect of gibberellin and auxin on parthenocarpic fruit growth induction in the cv Micro-Tom of tomato. *J. Plant Growth Regul.* **26**, 211–221.

Shahid, S., Kim, G., Johnson, N.R., Wafula, E., Wang, F., Coruh, C. *et al*. (2018) microRNAs from the parasitic plant *Cuscuta campestris* target host messenger RNAs. *Nature*, **553**, 82–85.

Shivaprasad, P.V., Chen, H., Patel, K., Bond, D.M., Santos, B.A.C.M. and Baulcombe, D.C. (2012) A microRNA superfamily regulates nucleotide binding site-leucine-rich repeats and other mRNAs. *Plant Cell*, **24**, 859–874.

da Silva, E.M., Silva, G.F.F.E., Bidoia, D.B., da Silva Azevedo, M., de Jesus, F.A., Pino, L.E., Peres, L.E.P. *et al*. (2017) microRNA159-targeted *SlGAMYB* transcription factors are required for fruit set in tomato. *Plant J.* **92**, 95–109.

Tamim, S., Cai, Z., Mathioni, S.M., Zhai, J., Teng, C., Zhang, Q. and Meyers, B.C. (2018) *Cis*-directed cleavage and nonstoichiometric abundances of 21-nucleotide reproductive phased small interfering RNAs in grasses. *New Phytol.* **220**, 865–877.

Tang, R., Zhou, Y., Chen, Z., Zeng, J., Huang, H., Jiang, Y.-M., Qu, H. *et al*. (2020) Involvement of miRNA-mediated anthocyanin and energy metabolism in the storability of litchi fruit. *Postharvest Biol. Technol.* **165**, 111200.

Tsuji, H., Aya, K., Ueguchi-Tanaka, M., Shimada, Y., Nakazono, M., Watanabe, R., Nishizawa, N.K. *et al*. (2006) GAMYB controls different sets of genes and is differentially regulated by microRNA in aleurone cells and anthers. *Plant J.* **47**, 427–444.

Tyler, L., Thomas, S.G., Hu, J., Dill, A., Alonso, J.M., Ecker, J.R. and Sun, T. (2004) DELLA proteins and gibberellin-regulated seed germination and floral development in *Arabidopsis*. *Plant Physiol.* **135**, 1008–1019.

Voinnet, O. (2009) Origin, biogenesis, and activity of plant microRNAs. *Cell*, **136**, 669–687.

Wang, X. and Chory, J. (2006) Brassinoteroids regulate dissociation of BKI1, a negative regulator of BRI1 signaling, from the plasma membrane. *Science*, **313**, 1118–1122.

Wang, H.-C., Lai, B. and Huang, X.-M. (2017) Litchi fruit set, development, and maturation. In *The Lychee Biotechnology*(Kumar, M., Kumar, V., Prasad, R. and Varma, A., eds), pp. 1–30. Singapore: Springer.

Wang, C., Jogaiah, S., Zhang, W., Abdelrahman, M. and Fang, J.G. (2018) Spatio-temporal expression of miRNA159 family members and their GAMYB target gene during the modulation of gibberellin-induced grapevine parthenocarpy. *J. Exp. Bot.* **69**, 3639–3650.

Xia, R., Meyers, B.C., Liu, Z., Beers, E.P., Ye, S. and Liu, Z. (2013) microRNA superfamilies descended from miR390 and their roles in secondary small interfering RNA biogenesis in eudicots. *Plant Cell*, **25**, 1555–1572.

Xia, R., Xu, J., Arikit, S. and Meyers, B.C. (2015) Extensive families of miRNAs and *PHAS* loci in Norway spruce demonstrate the origins of complex phasiRNA networks in seed plants. *Mol. Biol. Evol.* **32**, 2905–2918.

Xia, R., Chen, C., Pokhrel, S., Ma, W., Huang, K., Patel, P., Wang, F. *et al*. (2019) 24-nt reproductive phasiRNAs are broadly present in angiosperms. *Nat. Commun.* **10**, 1–8.

Ye, X., Wang, F. and Qian, N. (1992) Embryological studies of *Litchi chinensis*. *Acta Bot. Yunnanica* **14**, 59–65.

Yoshikawa, M., Peragine, A., Park, M.Y. and Poethig, R.S. (2005) A pathway for the biogenesis of *trans*-acting siRNAs in *Arabidopsis*. *Genes Dev.* **19**, 2164–2175.

Yu, S. and Wang, J.W. (2020) The crosstalk between microRNAs and gibberellin signaling in plants. *Plant Cell Physiol.* **61**, 1880–1890.

Yu, S., Galvao, V.C., Zhang, Y.-C., Horrer, D., Zhang, T.-Q., Hao, Y.-H. *et al*. (2012) Gibberellin regulates the *Arabidopsis* floral transition through miR156-targeted SQUAMOSA PROMOTER BINDING-LIKE transcription factors. *Plant Cell*, **24**, 3320–3332.

Yu, Y., Jia, T. and Chen, X. (2017) The 'how' and 'where' of plant microRNAs. *New Phytol.* **216**, 1002–1017.

Zhai, J., Jeong, D.H., de Paoli, E., Park, S., Rosen, B.D., Li, Y. *et al*. (2011) microRNAs as master regulators of the plant *NB-LRR* defense gene family via the production of phased, trans-acting siRNAs. *Genes Dev.* **25**, 2540–2553.

Zhang, X., Henriques, R., Lin, S.S., Niu, Q.W. and Chua, N.H. (2006) *Agrobacterium*-mediated transformation of *Arabidopsis thaliana* using the floral dip method. *Nat. Protoc.* **1**, 641–646.

Zhang, Y.C., Lei, M.Q., Zhou, Y.F., Yang, Y.W., Lian, J.P., Yu, Y. *et al*. (2020) Reproductive phasiRNAs regulate reprogramming of gene expression and meiotic progression in rice. *Nat. Commun.* **11**, 6031.

Zhang, Y., Waseem, M., Zeng, Z., Xu, J., Chen, C., Liu, Y., Zhai, J. *et al*. (2021) MicroRNA482/2118, a miRNA superfamily essential for both disease resistance and plant development. *New Phytol.* **233**, 2047–2057.

Zhao, Y., Wang, S., Wu, W., Li, L., Jiang, T. and Zheng, B. (2018) Clearance of maternal barriers by paternal miR159 to initiate endosperm nuclear division in *Arabidopsis*. *Nat. Commun.* **9**, 1–11.

Supporting information

Additional supporting information may be found online in the Supporting Information section at the end of the article.

Figure S1 Stem-loop of litchi miR482/2118 superfamily.
Figure S2 Expression of miR482/2118 and phasiRNAs from 23 *PHAS* genes triggered by miR482/2118 in litchi different organs.
Figure S3 Sequence similarity shown by alignment of *LITCHI007943* and two *LcGID1* genes.
Figure S4 *LcTASL*- and *LcGID1*-derived phasiRNA acted in *cis* on their precursor.
Figure S5 *LcTASL1*-derived 21-nt phasiRNAs cleaved *LcGID1*.
Figure S6 *LITCHI007944* (*LcTASL2*) is a long noncoding RNA (lncRNA).
Figure S7 Alignment of two *LcTASL* genes and *LcGID1B*.
Figure S8 *LcTASL1*-derived 21-nt phasiRNAs cleaved *LcTASL2*.
Figure S9 *LcTASL2*-derived 21-nt phasiRNAs cleaved *LcGID1*.
Figure S10 Expression pattern of key genes and associated sRNAs in the miR482/2118-*TASL*-phasiRNA-*GID1* pathway in various organs of 'HZ'.
Figure S11 Expression pattern of key genes and associated sRNAs in the miR482/2118-*TASL*-phasiRNA-*GID1* pathway during litchi cv. 'NMC' fruit development.
Figure S12 Prediction target site of *LcTASL1*-derived phasiRNAs on Arabidopsis *AtGID1*.
Figure S13 Prediction target site of *LcTASL2*-derived phasiRNAs on Arabidopsis *AtGID1*.
Figure S14 miR482/2118-*TASL*-*GID1* pathway constructed in *Arabidopsis*.
Figure S15 At-miR472 cleaved *LcTASL1* in 35S: *LcTASL1* transgenic lines.
Figure S16 Phenotypes of transgenic Arabidopsis plants.
Figure S17 Expression of four *LcGAMYB* genes in different development stages of 'NMC' seed.
Figure S18 Genome browser view of the distribution of the LcGAMYB33 binding peaks in the promoter and gene body of *LcTASL2*, *LcGID1C* and three *LcDELLA*.
Figure S19 Electrophoretic mobility shift assays (EMSAs) showing the binding ability of LcGAMYB33 with the mutant promoters of *LcMIR482e in vitro*.
Figure S20 *LcTASL1*-derived 22-nt phasiRNA cleaved *LcTASL2*.
Figure S21 Phenotype of litchi cv. 'Feizixiao' ('FZX') mature fruit.
Table S1 Revisiting miR482–2118 family in litchi.
Table S2 Revisiting target genes of miR482–2118 family in litchi.
Table S3 Revisiting *PHAS* loci of miR482–2118 family in litchi cv. 'HZ' different organs.
Table S4 Promoter analysis of key genes in the miR*482/2118-TASL-GID1-DELLA* pathway.
Table S5 Primers and probes used in this study.